ELSEVIER

Polymer 42 (2001) 4893–4901

polymer

www.elsevier.nl/locate/polymer

Mass transfer in rapidly photopolymerized poly(ethylene glycol) hydrogels used for chemical sensing

R.J. Russell, A.C. Axel, K.L. Shields, M.V. Pishko*

Department of Chemical Engineering, Texas A&M University, College Station, TX 77843-3122, USA

Received 11 September 2000; received in revised form 9 November 2000; accepted 13 November 2000

Abstract

Mass transfer in rapidly photopolymerized hydrogel networks of poly(ethylene glycol) (PEG) was investigated to characterize these materials for potential biosensor applications. The rapid polymerization from a concentrated polymer precursor solution results in a tightly cross-linked hydrogel network that potentially contains microgels, all conditions that can hinder analyte mass transfer. We examined the mass transfer characteristics of microspheres fabricated from diacrylated PEG (MW 575), dimethacrylated PEG (MW 1000), or tetra-acrylated PEG (MW 18,500) mixed with trimethylolpropane triacrylate, a triacrylated cross-linking agent, whose concentration ranged up to 20% (v/v). Swelling behavior was dynamically characterized starting from a dehydrated state using a CCD-camera integrated with an inverted microscope. Hydrogel swelling was extremely rapid with gel front diffusivities on the order of 10^{-6} cm^2/s. Estimated hydrogel mesh sizes ranged from 8.6 to 13.7 Å for spheres fabricated using PEG with molecular weights between 575 and 1000, to 103 Å for spheres fabricated using PEG with a molecular weight of 18,500. Dynamic uptake of tetramethylrhodamine was followed using a fluorescence microscope to estimate small analyte diffusivities into the hydrogel networks. Tetramethylrhodamine diffusivities were on the order of 10^{-7}–10^{-9} cm^2/s. Experimental diffusivities were used to simulate mass transfer into the gel and thus the potential response time of biosensors based on these systems.

Keywords: Poly(ethylene glycol); Microspheres; Penetrant diffusion

1. Introduction

Poly(ethylene glycol) (PEG) hydrogels are highly swollen matrices with demonstrated biocompatibility [1]. Numerous reports have appeared using PEG gels in drug delivery devices [2–8], for islet encapsulation [9], to prevent adhesions and inhibit thrombosis after surgery [10,11], and as a biocompatible surface treatment for cell adhesion-resistant surfaces [12,13]. Several researchers have examined thin films of PEG hydrogel networks fabricated from dilute solutions that were cross-linked using either low-energy light illumination with a photoinitiatior [14], with an electron beam [15] or gamma irradiation [4,16] of high molecular weight poly(ethylene oxide) (PEO) chains or chemically generated free-radical polymerizations of PEO chains for times as long as 24 h [17]. We have previously investigated the use of PEG hydrogels for electrochemical [18] and optical biosensing [19–21], drug delivery [22], patterned hydrogel microstructures [23] and as substrate materials for directed cell growth [24]. Many of these materials are formed by extremely rapid photopolymerizations from highly concentrated solutions of PEG acrylates.

Crosslinking in dilute polymer solutions should minimize the number of physical entanglements [25] and microgel formation from cyclic terminations during polymerization. Microgels are heterogeneities within the polymer network, the result of highly cross-linked polymer subdomains formed due to intrachain cyclization reactions [26–28]. These heterogeneities can reduce the overall cross-linking density of the hydrogel, as they do not contribute to the macroscopic network structure [29]. The PEG gels we have studied, whose fabrication requires polymerization on the order of seconds from highly concentrated PEG precursor solutions, may contain a large number of physical entanglements and microgels that influence mass transfer within the gel [22].

Several approaches to diffusion measurement in gels have appeared in the literature including side-by-side diffusion cells [4], uptake or release measurements into or from gels [30], dynamic light scattering [31] and patterned fluorescence correlation spectroscopy [32]. Merrill and coworkers have examined hydrogel uptake of proteins

* Corresponding author. Tel.: +1-979-847-9395; fax: +1-979-845-6446.
E-mail address: pishko@tamu.edu (M.V. Pishko).

0032-3861/01/$ - see front matter
PII: S0032-3861(00)00851-X

from a stirred solution using absorption spectroscopy [15] and by visually observing the diffusion of red-colored proteins through a PEG slab [33]. Kato and colleagues used anti-Stokes fluorescence imaging to trace a rhodamine B probe diffusing into and being released by a nonionic poly(*N*-isopropylacrylamide) gel [34].

Here we examine the mass transfer of water and small molecular weight fluorophore penetrants into these hydrogels. A CCD camera integrated with an inverted fluorescence microscope was used to examine both dynamic swelling behavior in water and uptake of a fluorescent dye in our PEG hydrogels. Measurements collected from analyzing these images were fit to an equation of motion for a swelling gel and conventional diffusion models to characterize the transport characteristics of these materials.

2. Experimental

2.1. Reagents

Tetramethylrhodamine isothiocyanate (TR), potassium phosphate monobasic, sodium phosphate dibasic, and sodium chloride were obtained from Sigma Chemical Co. (St. Louis, MO). Poly(ethylene glycol) diacrylate with a molecular weight of 575 (PEG-DA 575), trimethylolpropane triacrylate (TPT), and 2,2-dimethoxy-2-phenyl-acetophenone (DMPA) were obtained from Aldrich Chemical Co. (Milwaukee, WI). Poly(ethylene glycol) diacrylate with a molecular weight of 4000 (PEG-DA 4000) was obtained from Shearwater Polymers (Shearwater, FL). Poly(ethylene glycol) dimethacrylate with a molecular weight of 1000 (PEG-MA 1000) and tetrahydroxyl poly(ethylene glycol) bisphenol A bisepoxide with a molecular weight of 18,500 (PEG-18,500) were obtained from Polysciences (Warrington, PA). Light paraffin oil and *n*-heptane were purchased from Fisher Scientific, Inc. (Pittsburgh, PA). All reagents were used as received. One-tenth molar phosphate buffered saline (PBS, pH 7.4) was prepared from 1.1 mM potassium phosphate monobasic, 3 mM sodium phosphate dibasic heptahydrate, and 0.15 M NaCl in 18 MΩ cm deionized water (E-pure, Barnstead).

2.2. Preparation of tetraacrylated PEG 18,500

Tetraacrylated PEG-18,500 (PEG-TA-18,500) was prepared by acrylating the hydroxy functionalities of a tetrahydroxy PEG using a published protocol [35,36]. PEG-18,500 (20 g) was dissolved in 200 ml of dry benzene under nitrogen and heated at 40°C until fully dissolved. The solution was cooled in an ice bath, followed by addition of 0.7 ml of triethyl amine and 1.13 ml of acryloyl chloride. The mixture was then heated to reflux for 2 h, followed by stirring overnight at room temperature under nitrogen. The solution was filtered to remove the amine salts formed during the reaction and then the polymer was precipitated in *n*-heptane. The final product was isolated as a powder by subsequent drying at room temperature in a vacuum oven.

2.3. Preparation of PEG hydrogels

PEG-DA 575 hydrogels with 10% (v/v) crosslinking agent were synthesized as follows. TPT (100 μl) and 10 mg of DMPA were added to 1 ml of PEG-DA 575 and vortexed for 10 min. PEG precursor solutions were sprayed from a 23-gauge needle using an air compressor (model #DOA-P104-AA, Cole Parmer, Vernon Hills, IL) as shown in Fig. 1. Droplets of the precursor solution were sprayed into a two-phase liquid bath consisting of a top layer of *n*-heptane gently poured onto a layer of light mineral oil. The light mineral oil layer was illuminated with 365-nm light (20 W/cm^2) by an ultraviolet spot lamp (EFOS Ultracure 100SS Plus). DMPA photofragments upon exposure to the UV light resulted in the production of highly reactive radicals. These radicals induce gelation of the PEG chains into a hydrogel network by activating the PEG terminal acrylate or methacrylate groups. Gelled droplets were collected as cross-linked spheres at the bottom of the

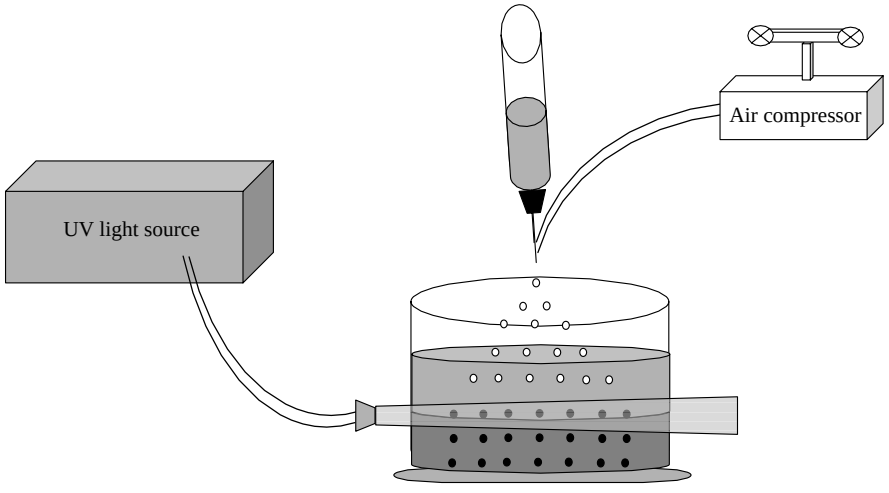

Fig. 1. PEG hydrogel microsphere fabrication. PEG precursor solutions were sprayed into a two-phase liquid bath of *n*-heptane upon light mineral oil. Spheres were cured via 365-nm illumination while descending through the light mineral oil phase.

mineral oil bath. The spheres were separated, rinsed in *n*-heptane to remove residual mineral oil, rinsed with 0.1 M PBS, and then dehydrated overnight in a vacuum oven at room temperature. Spheres were stored in the vacuum oven until examined to reduce humidity-induced swelling.

Additional spheres were fabricated by altering the amount of TPT added to the precursor solution (0, 10, and 20%), and changing the molecular weight of the PEG precursor from PEG-DA 575 to PEG-MA 1000, PEG-DA 4000, and PEG-TA 18,500. PEG-MA 1000, a waxy solid at room temperature, was heated to 37°C to melt the polymer before mixing the precursor solution. PEG-DA 4000 precursor solutions consisted of 200 mg of polymer powder dissolved per ml of PBS. PEG-TA 18,500 solutions consisted of 600 mg of polymer powder dissolved per ml of PBS.

2.4. Swelling measurements of hydrogels

A Zeiss Axiovert 135 fluorescence microscope equipped with an integrated CCD camera (Carl Zeiss Inc., Thornswood, NY) was used to observe the dynamic swelling of dehydrated PEG hydrogels. A 10× objective and a 10× eyepiece was used for all measurements. One to four spheres were placed on a microscope slide and exposed to ~100 μl of 0.1 M PBS. Optical images of sphere swelling were recorded at 5–10-min intervals using the Zeiss Image V3.0 software package. Observed radii changes were converted to pixel measurements using an objective micrometer slide and built-in data analysis subroutines. Pixel changes were then used to determine percent change in radius and an estimated swelling gel front diffusivity. Data from spheres that were physically moved by addition of the PBS (e.g. rolled or floated in the water) were disregarded.

Gel front diffusivity was determined using the equation of motion of a swelling gel network reported by Tanaka and coworkers [37]. The model describes the kinetics of spherical particles swelling in an aqueous solution by relating the time dependence of the change in gel radius to the viscoelastic properties of the gel network. The model assumes that the amount of swelling is sufficiently small such that Hooke's law can be applied to describe the elasticity of the gel network during swelling. The exact solution for swelling spherical gels under these conditions is then given by

$$u(r,t) = \sum_n F_n(r)\exp(-Dk_n^2 t)$$

where

$$F_n(r) = -6\Delta a_0 \frac{(-1)^n}{k_n a}\left[\frac{\cos(k_n r)}{k_n r} - \frac{\sin(k_n r)}{(k_n r)^2}\right]$$

and

$$k_n = n\pi/a$$

where $u(r,t)$ is the swelling displacement vector, D the swelling gel front diffusion coefficient, a the final sphere radius and Δa_0 the increase in sphere radius during swelling. This model was simulated with the infinite series truncated after the first 10 terms.

Swelling data was used to determine the average molecular weight between crosslinks M_c and average mesh size ζ following the approach first described by Flory. The Flory–Rehner equation [38] was used for calculations of homogeneous PEG hydrogels:

$$\frac{1}{M_c} = \frac{2}{M_n} - \frac{\frac{v}{V}(\ln(1-v_2) + v_2 + \chi v_2^2)}{v_2^{1/3} - \frac{v_2}{2}}$$

where M_c is the average molecular weight between crosslinks, M_n the number-average molecular weight of the uncross-linked polymer, V the molar volume of the solvent (18 cm^3/mol), v the specific volume of the solvent, v_2 the polymer volume fraction in the equilibrium swollen gel and χ the polymer–solvent interaction parameter. The sphere radii before and after hydration were used to calculate v_2. The polymer–solvent interaction parameter was estimated as 0.426. This value was reported to be nearly independent of PEG polymer volume fractions between 0.04 and 0.2 [15].

The Cima–Lopina modification to the Peppas–Merrill equation [5], shown below, was used to account for the introduction of the multi-functional TPT cross-linking agent:

$$\frac{1}{M_c} = \frac{2}{M_a} - \frac{\frac{v}{V}(\ln(1-v_{2,s}) + v_{2,s} + \chi v_{2,s}^2)}{v_{2,r}\left[\left(\frac{v_{2,s}}{v_{2,r}}\right)^{1/3} - \frac{v_{2,s}}{v_{2,r}}\left(\frac{2}{F_1} + \frac{1}{(M_a/M_c - 1)F_2}\right)\right]}$$

where M_a is the molecular weight of TPT, $v_{2,r}$ the polymer volume fraction of the gel after cross-linking but before swelling (i.e. 1), $v_{2,s}$ the polymer volume fraction of the swollen network, F_1 the PEG functionality, and F_2 the TPT functionality.

The average mesh size of the polymer network ξ was calculated as described by Merrill [15]. The root-mean squared end-to-end distance of a randomly coiled polymer chain of n bonds with a bond length l and characteristic ratio C_n was calculated as:

$$(r^2)^{1/2} = \chi C_n^{1/2} n^{1/2} l$$

where C_n is equal to 4.0, $l = 1.54$ Å and n is given by

$$n = 3M/44$$

where M is the molecular weight of the polymer chain (M_n). The average mesh size of the network is then given by

$$\zeta = v_2^{-1/3}(r^2)^{1/2}$$

2.5. Fluorescence measurements of hydrogels

Dynamic uptake of a fluorescent dye into hydrated PEG hydrogels was examined using the incident light fluorescence illumination subsystem of a Zeiss Axiovert

microscope. To prevent reactions between the isothiocyanate moiety and the PEG hydrogel, TR was dissolved in PBS at least one week prior to diffusion studies. The isothiocyanate moiety is known to be highly unstable in aqueous media and will rapidly hydrolyze [39]. A TR fluorescence filter with excitation and emission wavelengths of 540 ± 25 nm/605 ± 50 nm and a 565-nm bandsplitter was used to induce TR fluorescence. One to four fully hydrated spheres were placed on a microscope slide and exposed to ~100 μl of a TR-containing PBS solution (0.15 mM TR in 0.1 M PBS). Optical images of increasing sphere fluorescence were recorded at 5–10-min intervals using the Zeiss Image V3.0 software package. The shutter was closed between image capture events to minimize possible fluorophore photobleaching.

An estimated sphere diffusivity to small molecular weight penetrants was then calculated using established diffusion models for spheres [40]. The short-time behavior of penetrant diffusion in a solid can be most simply described by the following equation [41]:

$$\frac{M_t}{M_\infty} = kt^n$$

where M_t is the amount of penetrant in the sphere at time t, M_∞ the amount of penetrant uptake as time approaches infinity, k a coefficient describing influences of both the hydrogel network and the penetrant behavior and n, the diffusional exponent, is descriptive of the transport mechanism, i.e. whether diffusion is Fickian or anomalous. This model was used to determine the value of the diffusional exponent.

Diffusion coefficients were determined using the model shown below [40] where M_t is the amount of penetrant at time t, M_∞ the amount of penetrant uptake as time approaches infinity, D the diffusion coefficient and a the sphere radius:

$$\frac{M_t}{M_\infty} = 1 - \frac{6}{\pi^2}\sum_{n=1}^{\infty}\frac{1}{n^2}\exp(-Dn^2\pi^2 t/a^2)$$

This model describes the total amount of substance diffusing into a sphere, given that there is a constant surface concentration of diffusing material. Fluorescence intensity measurements were fit to the models using an iterative multi-variable regression algorithm for D and n. The infinite series was truncated after the first 10 terms.

The constant concentration surface boundary condition was verified by measuring the fluorescence of randomly positioned control regions in captured images of fluorescent spheres. A similar approach was used to discern when fluctuations in lamp intensity resulted in noisy data. Because of the inverted configuration of the fluorescence microscope, fluorescence was collected from both the sphere and a layer of TR-containing PBS under the sphere edges. The initial background fluorescence of individual spheres was therefore subtracted from all subsequent fluorescent images to show the increase in fluorescence in the sphere over its entire diameter.

3. Results and discussion

We have previously reported on microparticle hydrogel biosensors using rapidly photopolymerized hydrogel networks [20,21]. Spheres were formed from precursor solutions consisting of 70–100% diacrylated PEGs (where the remaining percentage consisted of an aqueous solution of protein dissolved into phosphate buffered saline). Exposure to the UV light necessary for photopolymerization was limited to seconds, to both minimize biomolecular exposure to the destructive UV light and to complete polymerization before the precursor solution droplets deformed from viscous resistance as they descended down the mineral oil column. The rapid polymerization from a concentrated solution results in a tightly cross-linked hydrogel network that potentially contains microgels, which can hinder mass transfer of analytes of sensing interest. Here we describe the mass transfer characteristics of hydrogel spheres formed from PEG macromolecules of differing molecular weight rapidly crosslinked from concentrated polymer solutions. Swelling behavior was characterized from a dehydrated state and the uptake of a fluorescent tracer was followed using a fluorescence microscope.

3.1. PEG hydrogels

PEG hydrogels prepared by spraying, regardless of PEG molecular weight and amount of cross-linker, were spherical in shape. While prior efforts using simple extrusion for droplet formation resulted in rapidly polymerized spherical gels, the resulting radii were typically 1–2 mm [20,21]. Spraying the precursor solutions prior to polymerization was expected to reduce the sphere size. The slight increase in air pressure is sufficient to offset the tendency of PEG solutions to form large droplets on the needle edge due to high surface tension. Spheres were sprayed into a two-phase liquid bath to alleviate problems with the air/mineral oil interfacial surface tension. When sprayed into pure mineral oil, the smallest droplets would spread over the mineral oil surface, due to low sphere weight and high surface tension of the mineral oil. When sprayed into the two-phase liquid, the sprayed PEG droplets easily penetrated into the *n*-heptane layer without distortion, but fell too rapidly through the beam of UV light for sufficient photopolymerization. The droplets were polymerized after descending into the more viscous light mineral oil layer. Spraying resulted in spheres an order of magnitude smaller than those generated with simple extrusion, although there was a high polydispersity in sphere size. This polydispersity is a direct function of the rate of extrusion. Precursor solutions extruded slowly with a consistent pressure, such as when using a syringe pump, resulted in the smallest and most uniform microspheres. Microspheres used for subsequent swelling and

diffusivity measurements were isolated by sieving and had dehydrated radii between 48 and 294 μm.

3.2. Characterization of PEG hydrogel hydration

Dynamic swelling measurements of the PEG hydrogels were obtained under an optical transmission microscope. The spheres swelled very rapidly, with most of the swelling completed within minutes. We found that 90% of the swelling for PEG DA 575 with 0% TPT was completed within 30 min. No additional swelling was observed when gels were allowed to hydrate overnight. Hydrogels fabricated from larger molecular weight PEGs required additional swelling time and underwent a larger percentage increase in diameter during hydration. For example, PEG-MA 1000 spheres with 0% TPT achieved 90% swelling after 40 min. PEG-TA 18,500 hydrogels continued to swell for as long as 4 h, with as much as a two-fold increase in diameter.

A similar preparation method for PEG hydrogel slabs has been reported by Scott and Peppas [3]. They explored cross-linked oligo(ethylene glycol) multiacrylates and acrylic acid slabs polymerized using bulk radical photopolymerization for 30 min. These polymer slabs experienced slow water uptake, with equilibrium swelling times as long as 100 h, likely due to the highly crosslinked nature of the polymer slabs.

Table 1 shows the calculated gel front diffusivities for the PEG hydrogels. The calculated diffusivities were all on the order of 10^{-6} cm^2/s. The experimentally determined diffusivity values are similar to those published for diffusion of unlinked PEG molecules in aqueous solution, where dilute solutions containing PEG 590 or 942 had diffusivities of 5.4×10^{-6} and 4.9×10^{-6} cm^2/s [42]. Values reported by Scott for PEG hydrogels fabricated with PEGs of molecular weights between 170 and 526 were on the order of 10^{-7}–10^{-8} cm^2/s, which accounted for the slower swelling behavior reported for those hydrogels. Increasing the amount of the cross-linking agent TPT resulted in a decrease in the calculated gel front diffusivity, as would be anticipated from the increase in hydrogel cross-linking and subsequent decrease in the molecular distance between cross-links.

Table 1
Influence of PEG molecular weight and cross-linker concentration on gel front diffusivities and change in sphere radii during hydration ($n > 10$)

Sphere type (PEG MW-% TPT)	Gel front diffusivity (cm^2/s) ($\times 10^6$)	Change in sphere radii upon hydration (%)
575-0	1.59 ± 0.42	16.2 ± 5.0
575-10	0.79 ± 0.18	5.2 ± 0.5
575-20	0.20 ± 0.09	5.9 ± 1.0
1000-0	5.12 ± 1.02	24 ± 2.9
1000-10	2.52 ± 0.72	16.5 ± 3.5
1000-20	1.85 ± 0.36	6.3 ± 1.0
18,000-0	3.43 ± 0.27	123 ± 9.0
18,000-10	2.52 ± 0.60	62.8 ± 4.3
18,000-20	1.22 ± 0.24	46 ± 3.1

The gel front diffusivity increased when using PEG-MA 1000 instead of PEG-DA 575, as would be expected from a greater distance between the cross-linked methacrylates. However, there was an unexpected decrease when the PEG molecular weight was increased from 1000 to 18,500. This is likely due to assumptions used in the derivation of the diffusivity model. The Tanaka model was originally derived for an elastic solid using Hooke's law [37]. PEG-TA 18,500 hydrogels experience more than a 100% change in radii, which is outside the model's predictive power. The large extent of hydrogel swelling likely invalidates using Hooke's law within the equation of motion. The currently applied model assumes a constant value for the friction coefficient between the hydrogel and the fluid f and the bulk K and shear modulus (μ) of the polymer network. A more accurate model would require modifying the equation of motion derived by Tanaka and coworkers to include K, μ and f as functions of both space and time and would require measuring these parameters throughout the swelling gel. However, while the PEG-TA 18,500 hydrogels experienced a slower swelling rate, they underwent a much greater change in volume than hydrogels prepared from the lower molecular weight PEGs.

The extent of sphere hydration is indicated in Table 1. As expected, spheres fabricated with tetraacrylated PEG-TA 18,500 molecules underwent the greatest change. PEG-TA 18,500 gels without any crosslinker experienced more than a two-fold increase in radii. The amount of swelling decreased with increasing amounts of TPT, due to formation of a tighter network. The extent of swelling increased with increasing PEG molecular weight due to the increased distance between cross-links.

The influence of PEG molecular weight and cross-linking agent on the average molecular weight between cross-links and mesh size is shown in Table 2. As one would anticipate from increasing the amount of cross-linking agent, there is a decrease in M_c for all three PEG molecular weights when additional amounts of TPT are added to the precursor solution. However, the decrease in ξ with additional cross-linking agent is small, except for the largest PEG

Table 2
Influence of PEG molecular weight and amount of cross-linking agent on hydrogel mesh size and average molecular weight between cross-links ($n > 10$)

Sphere type (PEG MW-% TPT)	M_c (g/mol)	Mesh size ζ (Å)
575-0	48	9.6
575-10	19	8.9
575-20	13	8.6
1000-0	104	13.7
1000-10	62	12.9
1000-20	20	11.7
18,500-0	3813.2	103.3
18,500-10	2710.1	95.1
18,500-20	755.0	76.2

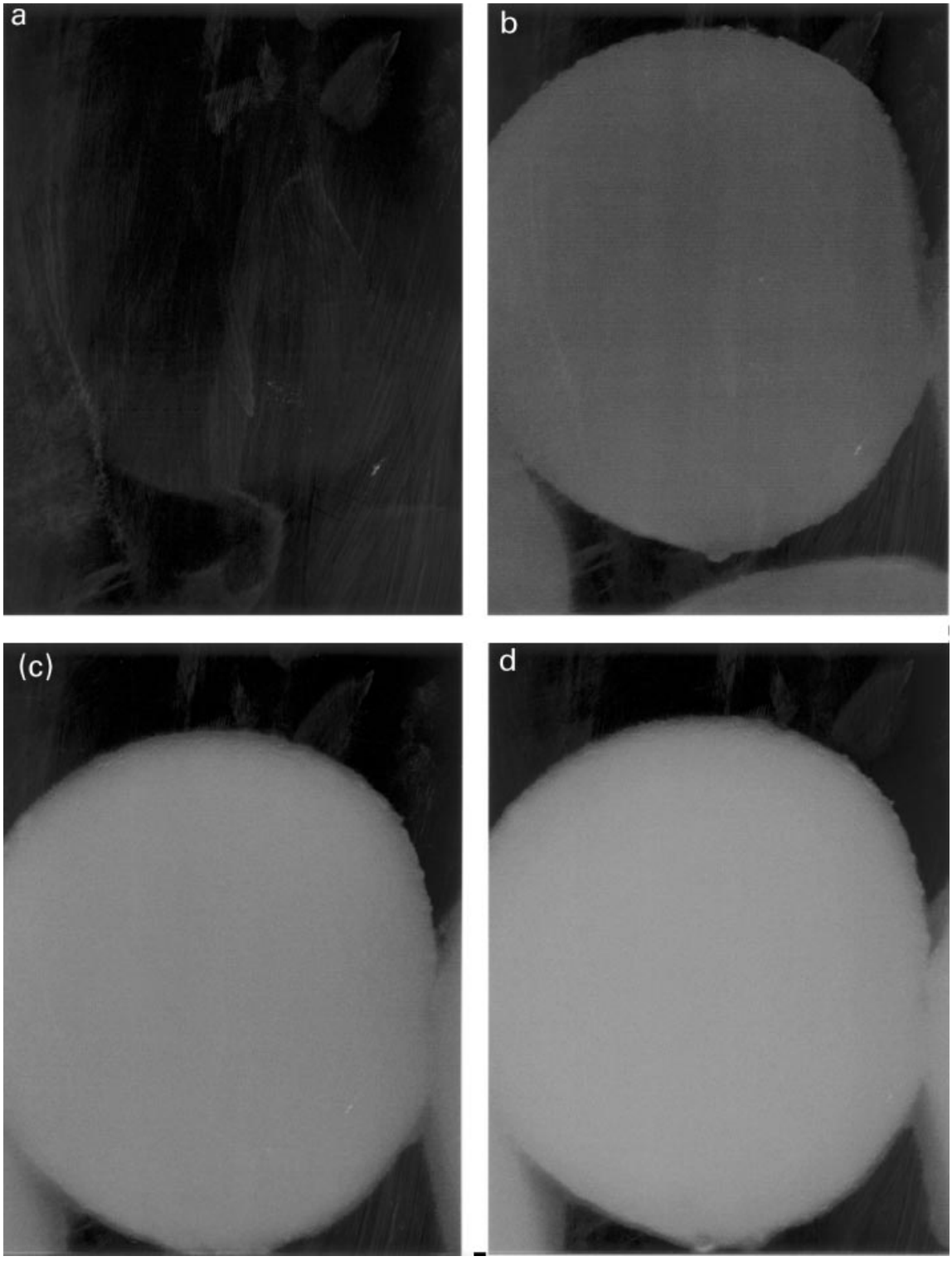

Fig. 2. Fluorescent micrographs of PEG-TA 18,500 spheres with 0% TPT: (a) before exposure to tetramethylrhodamine-containing solution; (b) 1 min; (c) 10 min and (d) 30 min after exposure. (Sphere size between 200 and 300 μm.)

molecular weight. It is worth noting that unlike PEG-DA 575 and PEG-MA 1000, which are linear, bifunctional molecules, PEG-TA 18,500 is a tetrafunctional molecule. In addition to cross-links between the α,ω acrylates, cross-linking of the two internal acrylates should result in regions with smaller molecular weights between cross-links and potential microgel formation. While crosslinking between the α,ω acrylates would result in an 18.5-kDa polymer loop, crosslinking between an α or ω acrylate with an internal acrylate would result in an approximately 9-kDa loop and

crosslinking between two internal acrylate groups would form a much smaller region between cross-links. Thus the calculated distance between cross-links is only an average of a more complicated macromolecular network structure.

It is also worth noting that the calculations for M_c and ξ are extremely sensitive to the value used for χ. Depending upon whether the mixing is exothermic or endothermic, the interaction parameter can take on values ranging both negative and positive and is frequently concentration dependant [43]. A χ value of 0.5 is indicative of an ideal system. Higher values indicate better mixing, while lower values favor phase separation [44]. Numerous values of χ, recently collected and reviewed by Amsden [45], have appeared in the literature. Most of the χ values for PEG have been determined for dilute solutions of PEG; these values were all ~0.5. While the χ value used in this work (0.426) has been reported to be independent of PEG volume fractions between 0.04 and 0.2, the polymer volume fractions observed in this work ranged between 0.09 and 0.86. Possible concentration-induced variations in the χ factor from that assumed in these calculations would thus result in proportional changes in the estimated mesh sizes. While the lack of precursor solution turbidity for the PEG–TPT–water solution may potentially indicate an interaction parameter without large deviations from 0.5, the calculated values reported in Table 2 should only be considered estimates.

3.3. Penetrant diffusivity into PEG hydrogels

The uptake of TR from 0.1 M PBS solution was used to estimate diffusion of small molecular weight penetrants into the PEG hydrogels. Penetrant diffusion is a critical parameter for many of the biosensing applications proposed for these hydrogels. Rapid diffusion of analytes such as glucose, lactate, and paraoxon, all compounds with molecular weights on the same order as TR (MW 444), is important for an acceptable sensor response time.

TR was selected as a fluorescent tracer because it is pH insensitive. As reported earlier, the cross-linked PEG hydrogel microenvironment is slightly acidic and results in an apparent pK_a shift of SNAFL-1, a fluorescein-based dye [21]. Initial investigations using fluorescein, a pH-sensitive dye, resulted in a diminished fluorescent response upon dye uptake due to the more acidic environment within the gels combined with the reduced quantum yield of fluorescein at acidic pH. In addition to being pH-insensitive, the photobleaching quantum yield of rhodamine dyes in PEG has been reported to be roughly the same as in water [46], which would reduce potential errors induced by differences in dye photobleaching rates between the buffer and hydrogel during TR uptake.

Images of hydrated spheres exposed to a TR-containing PBS solution were recorded on a fluorescent microscope using a 10× objective through a 10× eyepiece. Initial experiments indicated this objective had a fluorescent light collection depth sufficient for fluorescence profiling through the entire microsphere. An example of the diffusion of TR into a microsphere comprised of PEG-TA 18,500 with 0% TPT is pictured in Fig. 2. Cross-linked PEG-TA 18,500 spheres were exposed to and gradually were permeated by a solution containing TR. Initially, only scattered light made the sphere visible. Fluorescent TR diffusing into the spheres resulted in increased luminescence over 30 min shown in Fig. 2. Line and area-intensity profile measurement tools in Zeiss Image V3.0 were used to calculate fluorescent intensities as a function of time. These intensities were assumed proportional to the concentration of TR diffusing into the sphere. Depending upon the PEG MW and cross-linking concentration, TR uptake required as much as an hour to reach 90% of the steady-state fluorescence.

Additional swelling overnight did not result in increased fluorescence. As a control, a more concentrated solution of TR was used to verify that the highly fluorescent images were not corrupted by concentration quenching. Control regions integrated for fluorescent intensity over time verified the assumption of constant surface concentration. Spheres tested by stirring a larger solution of TR-containing PBS resulted in similar diffusion coefficient estimates indicating that solution-phase mass transfer resistance was negligible.

Estimated diffusion coefficients for TR uptake are shown in Table 3. For comparison, glucose in an aqueous solution has a diffusivity of approximately 6.8×10^{-6} cm^2/s [47]. TR diffusivity in water–methanol mixtures is on the order of 10^{-6} cm^2/s [32]. The diffusivity of TR through PEG-TA 18,500 with 0% TPT is 1.94×10^{-8} cm^2/s. Experimental diffusivity values were on the order of 10^{-8}–10^{-9} cm^2/s, similar to those reported by Scott for proxyphylline (MW 238) through short-chain PEGs. The experimentally determined diffusivities were smaller than those reported by Hubbell and coworkers for grafted PEG membranes with similar thicknesses [14]. Their films were constructed from dilute

Table 3
Diffusion coefficients of tetramethylrhodamine into cross-linked PEG hydrogels ($n > 8$)

Sphere type (PEG MW-% TPT)	TR diffusivity (cm^2/s) ($\times10^9$)	n
575-0	2.99 ± 0.20	0.45 ± 0.01
575-10	2.51 ± 0.14	0.44 ± 0.04
575-20	1.64 ± 0.07	0.44 ± 0.00
1000-0	13.90 ± 3.39	0.45 ± 0.01
1000-10	9.94 ± 3.98	0.47 ± 0.00
1000-20	6.53 ± 3.58	0.47 ± 0.01
4000-0	10.52 ± 1.50	0.47 ± 0.02
4000-10	7.50 ± 1.02	0.47 ± 0.01
4000-20	6.82 ± 1.03	0.46 ± 0.02
18,500-0	19.40 ± 5.31	0.52 ± 0.02
18,500-10	12.00 ± 3.21	0.44 ± 0.00
18,500-20	7.04 ± 3.04	0.44 ± 0.01

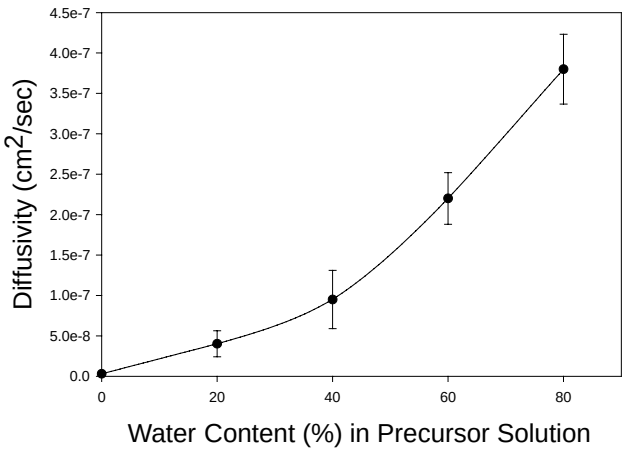

Fig. 3. Influence of precursor solution water content upon hydrogel diffusivity for PEG-DA 575 spheres with 0% TPT.

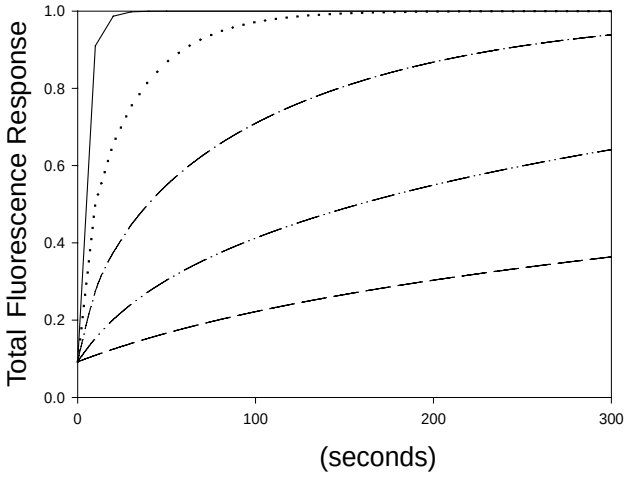

Fig. 4. Predicted response time for PEG hydrogel sensors constructed with PEG 18,500 and no TPT. (PEG microsphere radii are 10 (—), 25 (···), 50 (-·-), 100 (–···–···), and 200 μm (– –).

solutions containing only 10–30% PEG diacrylate and they noted there was a statistically significant decrease in diffusivity with increasing PEG concentrations. Films constructed rom dilute precursor solutions had diffusion coefficients for small analytes on the order of 10^{-6}–10^{-7} cm^2/s.

The calculated diffusion exponents indicate that the dominant diffusion mechanism was Fickian. With one exception, values calculated for *n* ranged between 0.44 and 0.47 as would be expected for nearly Fickian diffusion from a sphere or cylinder [41]. The lone exception was PEG-TA 18,500 without any cross-linking agent, which had a value of 0.52 for the diffusion exponent. This may be an indication of minor interaction between the penetrant and the polymer network resulting in slightly non-Fickian behavior.

The influence of increased water content in PEG-DA 575 precursor solutions is shown in Fig. 3. Hydrogel diffusivity increased two orders of magnitude as water content was increased. While PEG-DA 575 hydrogels (with no TPT added) had a TR diffusivity of 2.99×10^{-9} cm^2/s, spheres fabricated from a 80% water precursor solution had a diffusion coefficient of 3.8×10^{-7} cm^2/s. However, while increasing the water content had a pronounced effect upon the diffusion of small molecular weight analytes into the hydrogel, it also resulted in decreasing microsphere rigidity. Both the increased diffusivity and decreased rigidity are likely a direct result of decreased physical entanglements and increased cyclization, as similarly reported in previous studies and models of dimethacrylate polymerizations [48,49].

3.4. Simulated sensor response time

Penetrant diffusivities calculated above were used to determine sensor response time as a function of sphere size, assuming that the rate-limiting step was analyte diffusion into the hydrogel. The model described earlier for determining in the total amount of substance diffusing into a sphere was plotted as a function of sphere size. The most rapid predicted response (for hydrogels without increased water contents in the precursor solution) is shown in Fig. 4. Sensor response for hydrogel spheres fabricated from PEG-TA 18,500 with 0% TPT was calculated to be on the order of seconds to minutes when the sphere sizes are between 10 and 50 μm. Assuming the rate-limiting step is given by analyte diffusion into the sensor, the rapid responses necessary for many sensor applications would thus be possible using these hydrogels.

4. Conclusions

We have characterized the aqueous swelling and small penetrant diffusivities into rapidly cross-linked PEG hydrogel networks. The gels quickly obtain a high equilibrium water content and exhibit Fickian diffusion characteristics when exposed to diffusing tetramethylrhodamine dyes. Microsphere swelling behavior had gel front diffusivities on the order of 10^{-6} cm^2/s. While the diffusion coefficients of TR were on the order of 10^{-7}–10^{-9} cm^2/s, the values reported here demonstrate sufficiently rapid mass transfer for sensing applications as many proposed uses of these hydrogels involve micron-sized spheres and patterns that contain analyte sensitive recognition molecules [18,20,21].

Acknowledgements

The authors would like to acknowledge NASA-JSC (Contract #98-422), the National Science Foundation (BES-9908439), and the Texas Advanced Research Program for supporting the described work. R.R. received graduate support from the Paul and Ellen Deisler Endowed

Fellowship. M.V.P. acknowledges support from the Alfred P. Sloan Foundation through a research fellowship.

References

[1] Delgado C, Francis G, Fisher D. Crit Rev Ther Drug Carrier Syst 1992;9:249–304.
[2] West J, Hubbell J. React Polym 1995;25:139–47.
[3] Scott RA, Peppas NA. Biomaterials 1999;20:1371–80.
[4] Stringer J, Peppas N. J Control Release 1996;42:195–202.
[5] Keys KB, Andreopoulos FM, Peppas NA. Macromolecules 1998;31:8149–56.
[6] Gayet JC, Fortier G. J Control Release 1996;38:177–84.
[7] Hong S, Lee S, Lee Y, Chung S, Lee M, Shim C. J Control Release 1998;51:185–92.
[8] Jeong B, Bae YH, Kim SW. J Control Release 2000;63:155–63.
[9] Sawhney A, Pathak C, Hubbell J. Biomaterials 1993;14:1008–16.
[10] Hill-West J, Chowdhury S, Slepian M, Hubbell J. Proc Natl Acad Sci USA 1994;91:5967–71.
[11] Sawhney A, Pathak C, Rensburg JV, Dunn R, Hubbell J. J Biomed Mater Res 1994;28:831–8.
[12] Drumheller P, Hubbell J. J Biomed Mater Res 1995;29:207–15.
[13] Desai N, Hubbell J. J Biomed Mater Res 1991;25:829–43.
[14] Cruise GM, Scharp DS, Hubbell JA. Biomaterials 1998;19:1287–94.
[15] Merrill EW, Dennison KA, Sung C. Biomaterials 1993;14:1117–26.
[16] Lambov N, Stanchev D, Peikov P, Belcheva N, Stamenova R, Tsvetanov CB. Pharmazie 1995;50:126–8.
[17] Hassan CM, Doyle FJ, Peppas NA. Macromolecules 1997;30:6166–73.
[18] Sirkar K, Pishko MV. Anal Chem 1998;70:2888–94.
[19] Russell RJ, Pishko MV, Gefrides CC, Cote GL. Proc 20th Annu Int Conf IEEE Engng Medicine Biol Soc, 29 October–1 November 1998.
[20] Russell RJ, Pishko MV, Gefrides C, McShane M, Cote G. Anal Chem 1999;71:3126–32.
[21] Russell RJ, Pishko MV, Simonian AL, Wild JR. Anal Chem 1999;71:4909–12.
[22] Mellott MB, Searcy K, Pishko MV. Biomaterials 2001 (in press).
[23] Revzin A, Mellott M, Hile D, Kuo WG, Pishko M. Trans Sixth Word Biomater Congress, vol. I, 2000. p. 232.
[24] Ghosh P, Amirpour ML, Lackowski WM, Pishko MV, Crooks RM. Angew Chem Int Ed 1999;38:1592–5.
[25] Reinhart CT, Peppas NA. J Membr Sci 1984;18:227–39.
[26] Scott RA, Peppas NA. Macromolecules 1999;32:6139–48.
[27] Goodner MD, Bowman CN. Macromolecules 1999;32:6552–9.
[28] Kannurpatti AR, Bowman CN. Macromolecules 1998;31:3311–6.
[29] Elliott JE, Bowman CN. Macromolecules 1999;32:8621–8.
[30] Nguyen AL, Luong JHT. Biotechnol Bioengng 1986;28:1261–7.
[31] Westrin BA, Axelsson A, Zacchi G. J Control Release 1994;30:189–99.
[32] Hansen RL, Zhu XR, Harris JM. Anal Chem 1998;70:1281–7.
[33] Kofinas P, Athanassiou V, Merrill EW. Biomaterials 1996;17:1547–50.
[34] Kato E, Murakami T. Polym Gels Netw 1998;6:179–90.
[35] Quinn C, Pathak C, Heller A, Hubbell J. Biomaterials 1995;16:389–96.
[36] Pathak C, Sawhney A, Hubbell J. J Am Chem Soc 1992;114:8311–2.
[37] Tanaka T, Fillmore DJ. J Chem Phys 1979;70:1214–8.
[38] Flory PJ. Principles of polymer chemistry. Ithaca, NY: Cornell University Press, 1953.
[39] Brinkley M. Bioconjugate Chem 1992;3:2–13.
[40] Crank J. The mathematics of diffusion. 2nd ed. Oxford: Clarendon Press, 1975.
[41] Ritger PL, Peppas NA. Fuel 1987;66:815–26.
[42] Hamalainen KM, Kontturi K, Auriola S, Murtomaki L, Urtti A. J Control Release 1997;49:97–104.
[43] Kumar A, Gupta RK. Fundamentals of polymers. New York: McGraw Hill, 1998.
[44] McDaniels B. PhD dissertation, Texas A&M University (1999).
[45] Amsden B. Macromolecules 1999;32:874–9.
[46] Barnes MD, Ng KC, McNamara KP, Kung CY, Ramsey JM, Hill SC. Cytometry 1999;36:169–75.
[47] Longsworth LG. J Am Chem Soc 1952;74:4155–9.
[48] Landin DT, Macosko CW. Macromolecules 1988;21:846–51.
[49] Tobita H, Hamielec AE. Macromolecules 1989;22:3098–105.